PAPER

Theoretical analysis of dynamic processes for interacting molecular motors

IOP Publishing Journal of Physics A: Mathematical and Theoretical
J. Phys. A: Math. Theor. **48** (2015) 065001 (14pp) doi:10.1088/1751-8113/48/6/065001

Theoretical analysis of dynamic processes for interacting molecular motors

Hamid Teimouri, Anatoly B Kolomeisky and Kareem Mehrabiani

Department of Chemistry and Center for Theoretical Biological Physics, Rice University, Houston, TX 77005, USA

E-mail: tolya@rice.edu

Received 29 August 2014, revised 8 December 2014
Accepted for publication 10 December 2014
Published 21 January 2015

Abstract

Biological transport is supported by the collective dynamics of enzymatic molecules that are called motor proteins or molecular motors. Experiments suggest that motor proteins interact locally via short-range potentials. We investigate the fundamental role of these interactions by carrying out an analysis of a new class of totally asymmetric exclusion processes, in which interactions are accounted for in a thermodynamically consistent fashion. This allows us to explicitly connect microscopic features of motor proteins with their collective dynamic properties. A theoretical analysis that combines various mean-field calculations and computer simulations suggests that the dynamic properties of molecular motors strongly depend on the interactions, and that the correlations are stronger for interacting motor proteins. Surprisingly, it is found that there is an optimal strength of interactions (weak repulsion) that leads to a maximal particle flux. It is also argued that molecular motor transport is more sensitive to attractive interactions. Applications of these results for kinesin motor proteins are discussed.

Keywords: motor proteins, exclusion processes, stochastic models

(Some figures may appear in colour only in the online journal)

1. Introduction

A central role in supporting many cellular processes is played by several classes of enzymatic molecules that are known as motor proteins or molecular motors [1–5]. They use the chemical energy released from the hydrolysis of adenosine triphosphate (ATP) to drive cellular transport along cytoskeleton filaments. The single-molecule properties of various molecular

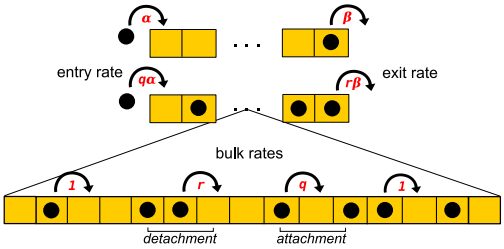

Figure 1. Schematic picture of the TASEP model with interacting particles.

motors have now been well investigated both experimentally and theoretically [4–6]. However, cellular cargoes are often moved by groups of motor proteins, and microscopic mechanisms of collective motor behaviors remain not well understood [5, 7, 8]. Recent experiments on kinesin motor proteins indicate that motors bound to the microtubule filament interact with each other [9–11]. The evidence for this behavior is found from observations that kinesins on microtubules phase segregate into more dense and less dense patches, and from measurements of different times of being bound to the filament depending on the presence of neighbors [9–11]. It was estimated that these interactions are weakly attractive $(1.6 \pm 0.5\, k_{\mathrm{B}}T)$ [9]. This raises the question of a fundamental role of this phenomenon in the collective motion of motor proteins. Various chemical transitions such as bindings, unbindings, hydrolysis and stepping should be affected by such potentials, influencing the overall dynamics of the motor proteins. However, the impact of such interactions on the transport of molecular motors has not been fully explored [7]. There are several investigations addressing the collective dynamics of interacting motor proteins [12–14, 24]. But the main limitation of these studies is a phenomenological description of interactions that does not provide a quantitative description for chemical transitions in motor proteins.

One of the most powerful tools in investigating multi-particle non-equilibrium systems is a class of models called totally asymmetric simple exclusion processes (TASEP) [15–17]. It is known that these models successfully capture essential properties of a large number of physical, chemical and biological systems [16–22]. Different versions of TASEP have been extensively employed in studies of various aspects of biological molecular motors [8, 13, 16, 19, 23, 24], providing important microscopic insights into these complex processes. TASEP with interactions have been studied before, but only for particles on a ring [13], or with phenomenologically defined interactions [24–26].

In this paper, we investigate the effect of inter-molecular interactions on the collective dynamics of motor proteins by introducing a new TASEP model with interactions. The most important advance of our method is that interactions are taken into account using a fundamental thermodynamic procedure. This provides a direct way of coupling microscopic properties of motor proteins with their collective dynamic features. To make the model more realistic, we use open boundary conditions, since the cytoskeleton filaments have finite length. Using various mean-field analytical methods and extensive Monte Carlo simulations, we compute particle currents and density profiles for molecular motors. This provides us with a direct method for addressing the fundamental role of the interactions. Our analysis suggests that there is an optimal interaction strength, corresponding to weak repulsions, that leads to the maximal particle flux. It is also found that interactions introduce significant correlations in the system and modify phase diagrams. In addition, the dynamic properties of molecular motors are influenced more strongly by attractive interactions.

2. The theoretical description

2.1. The model

We consider the transport of molecular motors on the cytoskeleton filaments as a multi-particle motion along a lattice segment with L sites, as illustrated in figure 1. The model assumes very long filaments, $L \gg 1$. For each lattice site i ($1 \leqslant i \leqslant L$), we assign an occupation number τ_i, where $\tau_i = 0$ if the site is empty and $\tau_i = 1$ if the site is occupied. Each site cannot be occupied by more than one particle. It is assumed that any two particles sitting on neighboring sites interact with each other with an energy E ($E > 0$ corresponds to attractions and $E < 0$ describes repulsions). A single motor that is not a part of the particle cluster can move forward with the rate 1 if it moves to the site without neighbors (figure 1). There is no energy change in this case. However, if the particle hops into another cluster, it moves with rate $q \neq 1$, because the energy of the system is changed by creating a new pair of neighbors (see figure 1). Similarly, for the particle breaking from the cluster, its forward rate is equal to $r \neq 1$ when the particle does not have neighbors in the new position. But for the case where one pair is broken and another one is created, the stepping rate is equal to 1, since there is no overall energy change (figure 1). Creating and breaking the pair of particles can be viewed as opposite chemical transitions, so detailed balance arguments can be applied:

$$\frac{q}{r} = \exp\left(\frac{E}{k_{\mathrm{B}}T}\right). \tag{1}$$

It is important to note that the stepping of the motor protein along the cytoskeleton filaments is a complex process that combines chemical transformations and mechanical motion. However, it can be viewed as a set of reversible chemical transitions between spatially separated biochemical states [3, 5]. For this reason, the stepping can be well approximated as a single reversible chemical reaction, justifying the application of the detailed balance arguments.

To simplify the analysis, we assume that the energy E is equally split between creation and breaking processes, providing explicit expressions for the stepping rates q and r:

$$q = \exp\left(\frac{E}{2k_{\mathrm{B}}T}\right), \quad r = \frac{1}{q} = \exp\left(\frac{-E}{2k_{\mathrm{B}}T}\right). \tag{2}$$

The splitting of the interaction potential between the rates q and r is not unique, but other possibilities can be easily explored in our method. In addition, it can be shown that one finds similar particle dynamics for all cases. Furthermore, our computer simulations (not shown here) indicate that the qualitative behavior of the system is independent of the energy splittings.

Equation (2) have a clear physical meaning. For attractive interactions ($E > 0$) the particle moves faster ($q > 1$), creating a new pair since the energy of the system decreases by E. Breaking out of the cluster increases the energy by E and the transition rate is slower ($r < 1$). Similar arguments can be given for repulsive interactions ($E < 0$). When there are no interactions ($E = 0$), we have $q = r = 1$, and the original TASEP case with only hard-core exclusions is recovered.

This model is related to a class of lattice-gas models studied by Katz, Lebowitz and Spohn, which are known as KLS models [26, 27]. The KLS model approach has been employed for gaining an understanding of the non-equilibrium properties of multi-particle systems. However, our method is not the same as the KLS model approach. The main difference is that our transition rates are determined from fundamental thermodynamic

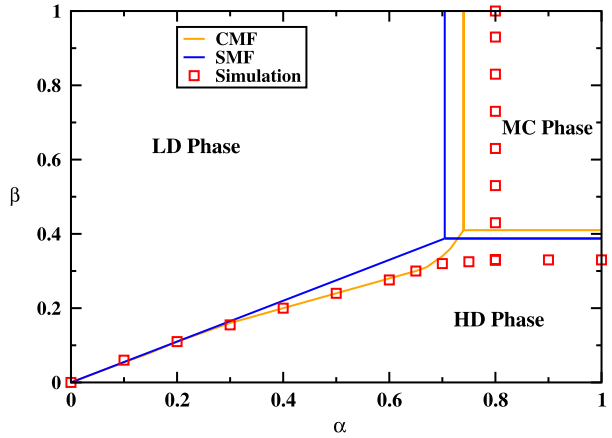

Figure 2. Stationary phase diagram for TASEP with inter-molecular interactions. The case of weakly repulsive interactions, $E = -1.2\ k_B T$, is shown.

arguments, while the KLS models are generally inconsistent with the thermodynamics. It is important to emphasize that, generally, stochastic models are not derived from first principles. So their applications for real systems in chemistry, physics and biology must be accompanied by fundamental constraints. The requirement of thermodynamic consistency is such a constraint. This is the main factor preventing the KLS models from being used for analyzing interactions in motor proteins, although they are still important for clarifying general principles for non-equilibrium systems. Furthermore, the importance of thermodynamic constraints can be seen from the fact that the number of possible stationary phases decreases in comparison with the KLS model predictions, as we show below. At the same time, for weak interactions the two approaches converge, as expected. We also note here that, in contrast to the methods of some previous studies, our thermodynamically consistent method accounts for interactions in *all* chemical transitions in the system. In addition, it differs from other TASEP with interactions [13, 24, 25, 29, 30], because in our model the stepping rates depend on the states of four consecutive lattice sites.

Interactions also modify the boundary transitions as shown in figure 1. The entrance rate is equal to α if no particle pair created, while the rate is equal to $q\alpha$ when pair creation is involved. Similarly, the exit rate for the single particle is given by the rate β, while exiting with breaking from the cluster changes the rate to $r\beta$.

2.2. Simple mean-field theory

To analyze the system, we start with the simplest mean-field (SMF) approach, which neglects all correlations in the system. It assumes that for any two sites on the lattice, their occupancies are independent of each other, i.e., $\mathrm{Prob}(\tau_i, \tau_j) \approx \mathrm{Prob}(\tau_i) * \mathrm{Prob}(\tau_j)$ for $1 \leqslant i, j \leqslant L$. The particle density at every site is associated with an average occupancy, $\rho = \langle \tau \rangle$, and it reaches a constant value in the bulk of the system. It can be shown that, like for the classical TASEP without interactions, there are three stationary phases: low density (LD), high density (HD) and maximal current (MC), as illustrated in figure 2.

When the dynamics at the entrance is rate-limiting, we have an LD phase. In this case the temporal evolution of the particle density ρ at every lattice site can be described by

$$\frac{\mathrm{d}\rho}{\mathrm{d}t} = \alpha(1-\rho)^2 + q\alpha\rho(1-\rho) - \rho(1-\rho)^3 - r\rho^2(1-\rho)^2 - \rho^3(1-\rho) - q\rho^2(1-\rho)^2. \tag{3}$$

This equation suggests that the change in the particle density is determined by the difference in the particle fluxes. The first two terms on the right-hand side correspond to the entrance current, while the last four terms are for the bulk current that leaves the giving lattice site. For the stationary state, we have $\frac{\mathrm{d}\rho}{\mathrm{d}t} = 0$, and this equation can be solved exactly, producing the following expression:

$$\rho_{\mathrm{LD}} = \frac{q - \sqrt{q^2 - 4\alpha q(q-1)}}{2(q-1)}. \tag{4}$$

For $q = 1$ this reduces to $\rho_{\mathrm{LD}} = \alpha$, as expected for the standard TASEP without interactions. From this equation and using equation (3), the expression for the current can be also derived:

$$J_{\mathrm{LD}} = \alpha\,\frac{\alpha q(q-1) - 1 + \sqrt{q^2 - 4\alpha q(q-1)}}{q-1}, \tag{5}$$

which in the limit $q \to 1$ produces $J_{\mathrm{LD}} = \alpha(1-\alpha)$.

For the case where the exiting becomes the rate-limiting step, the system is in an HD phase. In this case, the time evolution of the particle density is given by

$$\frac{\mathrm{d}\rho}{\mathrm{d}t} = \rho(1-\rho)^3 + r\rho^2(1-\rho)^2 + \rho^3(1-\rho) + q\rho^2(1-\rho)^2 - \beta\rho(1-\rho) - r\beta\rho^2. \tag{6}$$

For the steady-state limit, we obtain

$$\rho_{\mathrm{HD}} = \frac{q - 2 + \sqrt{q^2 - 4\beta(q-1)}}{2(q-1)}, \tag{7}$$

while for the current we have

$$J_{\mathrm{HD}} = \beta\,\frac{\beta(q-1) - 1 + \sqrt{q^2 - 4\beta(q-1)}}{q(q-1)}. \tag{8}$$

When there are no interactions in the system ($q = 1$), the particle density and the current reduce to the values for the standard TASEP: $\rho_{\mathrm{HD}} = 1 - \beta$ and $J_{\mathrm{HD}} = \beta(1-\beta)$.

In the bulk of the system, the steady-state particle current is independent of the entry and exit rates. It can be expressed in terms of an average density ρ in the following form:

$$J = \rho(1-\rho)^3 + r\rho^2(1-\rho)^2 + \rho^3(1-\rho) + q\rho^2(1-\rho)^2, \tag{9}$$

where $q = \frac{1}{r} = \exp\left(\frac{E}{2k_{\mathrm{B}}T}\right)$. In this situation, the current can reach its highest value, and this phase is known as a maximal current (MC) phase. For the case of no interactions ($E = 0$ and $q = r = 1$), we obtain the parabolic expression $J = \rho(1-\rho)$ for the current, as expected for the standard TASEP model without interactions. The MC phase is specified by the condition that $\frac{\partial J}{\partial \rho} = 0$, which leads to the following expression:

$$(2\rho - 1)\Big[-1 + \rho(4 - 2q - 2r) + \rho^2(2r + 2q - 4)\Big] = 0. \tag{10}$$

This equation has only one real root: $\rho = \frac{1}{2}$. Substituting $\rho = \frac{1}{2}$ into equation (9), we obtain the following expression for the maximal current as a function of the interaction energy:

$$J_{\mathrm{MC}} = \frac{1}{8} + \frac{r+q}{16} = \frac{1}{8} + \frac{\exp\left(\frac{E}{2k_{\mathrm{B}}T}\right) + \exp\left(\frac{-E}{2k_{\mathrm{B}}T}\right)}{16}. \tag{11}$$

For $E = 0$ ($q = r = 1$) it yields $J_{\mathrm{MC}} = \frac{1}{4}$, as expected for the standard TASEP model without interactions. In the MC phase the bulk density reaches the maximal value of $\rho_{\mathrm{MC}} = 1/2$.

Our computer simulations indicate that LD–MC and HD–MC transitions are continuous. We use then the continuity of the stationary current at the transition to determine the boundary lines separating LD and MC and HD and MC phases. The equality of the stationary current at the boundary $J_{\mathrm{MC}} = J_{\mathrm{LD}}$ yields the following expression:

$$\alpha(1-\rho)^2 + q\alpha\rho(1-\rho) = \rho(1-\rho)^3 + r\rho^2(1-\rho)^2 + \rho^3(1-\rho) + q\rho^2(1-\rho)^2. \tag{12}$$

Since in the MC phase the density is equal to $\rho = 1/2$, the boundary in terms of the entrance rate is given by

$$\alpha_{\mathrm{b}} = \frac{1+q}{4q}. \tag{13}$$

Similarly, we can determine the boundary between the HD and MC phases:

$$\beta_{\mathrm{b}} = \frac{1+q}{4}. \tag{14}$$

However, the transition between the LD and HD phases is discontinuous and it involves a density jump. Then, from the condition of equal current at the phase line: $J_{\mathrm{HD}} = J_{\mathrm{LD}}$, we derive

$$\beta\rho_{\mathrm{HD}}\left(1-\rho_{\mathrm{HD}}\right) + r\beta\rho_{\mathrm{HD}}^2 = \alpha\left(1-\rho_{\mathrm{LD}}\right)^2 + q\alpha\rho_{\mathrm{LD}}\left(1-\rho_{\mathrm{LD}}\right). \tag{15}$$

Using equations (4) and (7), it can be shown that this leads to a simple relation for this phase boundary:

$$\beta = q\alpha. \tag{16}$$

2.3. Cluster mean-field theory

The fact that the SMF method neglects correlations is the main reason for it not yielding a satisfactory description of TASEP with stronger inter-molecular interactions. To develop a more reasonable analysis, we propose to use a mean-field approach that takes into account some correlations. Our idea is to fully describe the particle dynamics inside a cluster of several lattice sites, but neglecting correlations between states of different clusters. In our calculations, clusters with two lattice sites are utilized. In this approach, the occupation of four consecutive sites is written as $\mathrm{Prob}(\tau_{i-1}, \tau_i, \tau_{i+1}, \tau_{i+2}) \approx \mathrm{Prob}(\tau_{i-1}, \tau_i) * \mathrm{Prob}(\tau_{i+1}, \tau_{i+2})$. The method is called a cluster mean-field (CMF) method. There are four possible states for each two-site cluster depending on the occupancy of the sites, which can be labeled as (1, 1), (1, 0), (0, 1) and (0, 0). We define P_{11}, P_{10}, P_{01} and P_{00} as the probabilities of the cluster being found in each of these configurations, respectively. The normalization requires that $P_{11} + P_{10} + P_{01} + P_{00} = 1$. The average bulk density and the current can be expressed in terms of these functions:

$$\rho_{\text{bulk}} = \frac{1}{2}\sum_{\tau_1}\sum_{\tau_2}\tau_1 P(\tau_1, \tau_2) + \frac{1}{2}\sum_{\tau_1}\sum_{\tau_2}\tau_2 P(\tau_1, \tau_2)$$
$$= \frac{1}{2}\sum_{\tau_1}\sum_{\tau_2}\left[\tau_1 P(\tau_1, \tau_2) + \tau_2 P(\tau_1, \tau_2)\right]$$
$$= P_{11} + \frac{P_{01} + P_{10}}{2}. \tag{17}$$

In the CMF, all dynamic properties for TASEP with interactions can be obtained by analyzing changes of cluster probabilities with time. The temporal evolution of two-site probabilities in the bulk is governed by a set of master equations:

$$\frac{\mathrm{d}P_{11}}{\mathrm{d}t} = qP_{01}P_{01} + P_{11}P_{01} - rP_{11}P_{00} - P_{11}P_{01}; \tag{18}$$

$$\frac{\mathrm{d}P_{00}}{\mathrm{d}t} = qP_{01}P_{01} + P_{11}P_{01} - rP_{11}P_{00} - P_{11}P_{01}; \tag{19}$$

$$\frac{\mathrm{d}P_{01}}{\mathrm{d}t} = P_{10}\Big[P_{10}P_{01} + P_{00}^2 + P_{00}P_{01} + P_{00}P_{10}\Big] + rP_{10}\Big[P_{11}P_{00} + P_{01}^2 + P_{00}P_{01} + P_{01}P_{11}\Big]$$
$$+ P_{10}\Big[P_{10}P_{11} + P_{11}^2 + P_{11}P_{01} + P_{01}P_{10}\Big] + qP_{10}\Big[P_{00}P_{10} + P_{10}^2 + P_{11}P_{10} + P_{00}P_{11}\Big]$$
$$- P_{01}\Big[qP_{00}P_{01} + P_{00}^2 + P_{00}P_{10} + qP_{10}P_{01} + P_{00}P_{01} + qP_{01}^2 + P_{00}P_{11} + qP_{11}P_{01}\Big]$$
$$- P_{01}\Big[qP_{11}P_{01} + P_{11}^2 + P_{11}P_{10} + qP_{10}P_{01} + qP_{01}^2 + P_{00}P_{11} + P_{11}P_{01} + qP_{00}P_{01}\Big]; \tag{20}$$

$$\frac{\mathrm{d}P_{10}}{\mathrm{d}t} = 2rP_{11}P_{00} + P_{01}P_{00} + P_{01}P_{11} - P_{10}\Big[P_{10}P_{01} + P_{00}^2 + P_{00}P_{01} + P_{00}P_{10}\Big]$$
$$- rP_{10}\Big[P_{11}P_{00} + P_{01}^2 + P_{00}P_{01} + P_{01}P_{11}\Big] - P_{10}\Big[P_{10}P_{11} + P_{11}^2 + P_{11}P_{01} + P_{01}P_{10}\Big]$$
$$- qP_{10}\Big[P_{00}P_{10} + P_{10}^2 + P_{11}P_{10} + P_{00}P_{11}\Big]. \tag{21}$$

From equation (18), for the stationary state we obtain

$$qP_{01}^2 = rP_{11}P_{00}, \tag{22}$$

while equations (20) and (21) yield

$$P_{10}^2\big[P_{01}(2 - r - q) + q\big] + P_{10}\big[P_{00} + P_{11} + rP_{01} + P_{00}P_{11}(q + r - 2)\big]$$
$$- 2qP_{01}^2 - P_{00}P_{01} - P_{11}P_{01} = 0. \tag{23}$$

So far, we have three equations with four unknown two-site cluster probabilities, and we need one more. The last equation can be derived from the expression for the current:

$$J = qP_{01}^2 + rP_{11}P_{00} + P_{11}P_{01} + P_{00}P_{01} = 2rP_{11}P_{00} + \sqrt{P_{11}P_{00}}\big(P_{00} + P_{11}\big), \tag{24}$$

where equation (22) was used to eliminate P_{01}. Using the normalization condition, the average density from equation (17) can be written as

$$\rho = \frac{1}{2}\big(1 + P_{11} - P_{00}\big). \tag{25}$$

Now we can define a new variable η such that

$$\eta = P_{11} + P_{00}. \tag{26}$$

Then the particle current can be expressed as a function of ρ and η. Then, applying the condition of maximal current, $\nabla J(\rho, \eta) = 0$, it can be shown that $\rho = \frac{1}{2}$. This suggests that $P_{11} = P_{00} = qP_{01}$. Utilizing this condition together with the normalization, we obtain the following cubic equation for P_{01}:

$$P_{01}^3\Big[-1 - 2q + 2q^2 + 4q^3 - q^4 - 2q^5\Big] + P_{01}^2\Big[1 - 2q - 10q^2 + 2q^3 + 5q^4\Big] + P_{01}\Big[2q - q^2 - 4q^3\Big] + q^2 = 0. \tag{27}$$

The physically reasonable root ($0 < P_{01} < 1$) of this equation can be found, and it is used then to calculate the current via the relation $J = 4qP_{01}^2$. Various cluster probabilities can be interpreted as measures of clustering in the lattice. For very strong repulsion, $P_{11} \to 0$ and no clusters form. As the interaction energy becomes more attractive, P_{11} increases and the particles then have a larger tendency to form clusters.

At the entrance, the cluster probabilities satisfy the following master equations:

$$\frac{\mathrm{d}P_{11}}{\mathrm{d}t} = q\alpha P_{01} - rP_{11}P_{00} - P_{11}P_{01}; \tag{28}$$

$$\frac{\mathrm{d}P_{00}}{\mathrm{d}t} = P_{00}P_{01} + qP_{01}P_{01} - \alpha P_{00}; \tag{29}$$

$$\frac{\mathrm{d}P_{10}}{\mathrm{d}t} = \alpha P_{00} + rP_{11}P_{00} + P_{11}P_{01} - P_{10}\Big[P_{00} + P_{01} + qP_{11} + qP_{10}\Big]; \tag{30}$$

$$\frac{\mathrm{d}P_{01}}{\mathrm{d}t} = P_{10}\Big[P_{00} + P_{01} + qP_{11} + qP_{10}\Big] - q\alpha P_{01} - P_{00}P_{01} - qP_{01}P_{01}. \tag{31}$$

For the stationary state, it can be shown that

$$P_{00} = \frac{qP_{01}^2}{\alpha - P_{01}}, \tag{32}$$

$$P_{11} = q\big(\alpha - P_{01}\big), \tag{33}$$

and

$$qP_{10}^2 + P_{10}\Big(P_{00} + P_{01} + qP_{11}\Big) - q\alpha P_{01} - \alpha P_{00} = 0. \tag{34}$$

Using the normalization condition: $P_{10} = 1 - \mathrm{P}_{00} - \mathrm{P}_{11} - P_{01}$, we obtain

$$P_{01}^2(q-1) + P_{00}^2(q-1) - qP_{11} + P_{00}(1-2q) + P_{01}(1-2q) + P_{11}P_{00}(q-1) + P_{11}P_{01}(q-1) + 2P_{00}P_{01}(q-1) + q - q\alpha P_{01} - \alpha P_{00} = 0. \tag{35}$$

Then from equations (32) and (33), we derive the final expression for P_{01}:

$$\begin{aligned} &P_{01}^4\left(2q^3-5q^2+4q-1\right)+P_{01}^3\left(-2\alpha q^3+7\alpha q^2+3q^2-7q\alpha-3q+2\alpha+1\right)\\ &+P_{01}^2\left(\alpha^2q^3-4\alpha^2q^2-5\alpha q^2+5\alpha^2q+5q\alpha+q-\alpha^2-2\alpha\right)\\ &+P_{01}\left(\alpha^3q^2+3\alpha q^2-2q\alpha^3-2q\alpha^2-2q\alpha+\alpha^2\right)\\ &+q\alpha^2-q^2\alpha^3=0. \end{aligned} \tag{36}$$

This can be solved numerically, leading to the calculation of all of the other properties in the LD phase.

In the HD phase, the exit is controlling the dynamics, and cluster probabilities evolve as follows:

$$\frac{\mathrm{d}P_{11}}{\mathrm{d}t}=qP_{01}P_{01}+P_{11}P_{01}-r\beta P_{11}; \tag{37}$$

$$\frac{\mathrm{d}P_{00}}{\mathrm{d}t}=\beta P_{01}-rP_{11}P_{00}-P_{00}P_{01}; \tag{38}$$

$$\frac{\mathrm{d}P_{01}}{\mathrm{d}t}=P_{10}\left[P_{00}+P_{10}+rP_{11}+rP_{01}\right]-P_{11}P_{01}-qP_{01}P_{01}-\beta P_{01}; \tag{39}$$

$$\frac{\mathrm{d}P_{10}}{\mathrm{d}t}=P_{01}P_{00}+rP_{11}P_{00}+r\beta P_{11}-P_{10}\left[P_{00}+P_{10}+rP_{11}+rP_{01}\right]. \tag{40}$$

For the steady state, we obtain

$$P_{11}=\frac{qP_{01}^2}{r\beta-P_{01}}, \tag{41}$$

$$P_{00}=\beta-qP_{01}, \tag{42}$$

and

$$P_{10}^2+P_{10}\left[P_{00}+rP_{11}+rP_{01}\right]-\beta rP_{11}-\beta P_{01}=0. \tag{43}$$

Again using the normalization condition, one can calculate

$$\begin{aligned} &P_{01}^2(1-r)+P_{00}^2(1-r)+P_{11}(r-2)-P_{00}+P_{01}(r-2)+P_{11}P_{00}(1-r)\\ &\quad+P_{00}P_{01}(1-r)+2P_{11}P_{01}(1-r)+1-\beta P_{01}-r\beta P_{11}=0. \end{aligned} \tag{44}$$

Eliminating P_{00} and P_{11} from this expression yields

$$\begin{aligned} &P_{01}^4\left(2q^5-5q^4+4q^3-q^2\right)+P_{01}^3\left(3q^4-3q^3+q^2+2q\beta-7q^2\beta+7\beta q^3-2\beta q^4\right)\\ &+P_{01}^2\left(q^3-\beta^2+q^3\beta^2-5\beta q^3-3q^2\beta^2+5\beta q^2+4q\beta^2-2q\beta\right)\\ &+P_{01}\left(\beta^2-\beta^3-2q\beta^2-2\beta q^2+3\beta^2q^2\right)\\ &+q\beta^2-q\beta^3=0. \end{aligned} \tag{45}$$

This equation can be solved numerically exactly for P_{01}, and all of the other properties can be obtained as explained above.

The phase diagram for the CMF method can be obtained using the same approach as was explained for the SMF method. We apply the condition $J_{\mathrm{LD}}=J_{\mathrm{MC}}$ to determine the boundary between the LD and MC phases:

$$\alpha P_{00} + q\alpha P_{01} = qP_{01}P_{01} + rP_{11}P_{00} + P_{11}P_{01} + P_{00}P_{01}. \tag{46}$$

For the MC phase, we have $\rho_{\text{bulk}} = 0.5$, and this leads to $P_{11} = P_{00}$. Combining this equality with equations (32) and (33), the following quadratic equation is derived:

$$\alpha^2 - 4\alpha P_{01} + 4P_{01}^2 = 0. \tag{47}$$

It has only one solution: $\alpha_{\text{b}} = 2P_{01}$, where P_{01} is the solution of equation (27). Similarly, for the boundary between the HD and MC phases, we obtain $\beta_{\text{b}} = 2qP_{01}$. To determine the phase boundary between the LD and HD phases we must solve the equation $J_{\text{LD}} = J_{\text{HD}}$, producing

$$\alpha P_{00} + q\alpha P_{01} = \beta P_{01} + r\beta P_{11}. \tag{48}$$

This can be further simplified to

$$\beta^2\left(P_{01} - \alpha\right) + q\alpha^2\beta - q^2\alpha^2 P_{01} = 0. \tag{49}$$

Solving this equation for β leads us to

$$\beta = \frac{q\alpha P_{01}}{\alpha - P_{01}}. \tag{50}$$

From equation (50), it can be shown that $P_{01} = \frac{\alpha\beta}{q\alpha+\beta}$. After substituting this into equation (36), we obtain the following relation for the boundary between the LD and HD phases:

$$\begin{aligned}\beta^4(1-q) + \beta^3(-1 + 3\alpha + 2q - 2q\alpha) + \beta^2\Big(-\alpha + \alpha^2 - q + q\alpha + q\alpha^2 \\ + 2q^2\alpha + q^2\alpha^2 - q^3\alpha^2) + \beta\Big(-q\alpha^2 - 2q^2\alpha + 2q^2\alpha^2 + 2q^2\alpha^3 + q^3\alpha^2 - q^3\alpha^3\Big) \\ - q^3\alpha^2 + q^4\alpha^3 = 0.\end{aligned} \tag{51}$$

3. Monte Carlo simulations and discussion

We performed extensive Monte Carlo simulations to test our theoretical predictions. Our chosen lattice size, $L = 1000$, is large enough for avoiding finite size and boundary effects. A random sequential update was utilized for all simulations. The particle current and density profiles were averaged over 10^8 Monte Carlo steps and the first 20% were discarded to ensure that the system had reached the steady state. Comparing theoretical predictions from the SMF approach with Monte Carlo computer simulations (figures 2 and 3), we can see that it provides a reasonable approximation for very weak interactions ($E \approx 0$), while for stronger attractions or repulsions the simple mean-field method does not work well. The calculated density profiles in the SMF approach deviate from computer simulation results (see figure 3). But the strongest argument against using the SMF for TASEP with interactions comes from the analysis of equation (11) for the current in the MC phase. It predicts that for $|E| \gg 1$ the current is increasing without bound, which is clearly an unphysical result. In the case of strong attractions, particles will tend to stay in one big cluster that cannot move because particle breaking from the cluster is not possible. In this case the current is expected to go to zero. For strong repulsions, the situation is different. In this case any particle cannot have neighbors, so the system behaves like TASEP with particles that cover two sites, for which precise estimates for the current are known: $J = 1/(\sqrt{2} + 1)^2 \approx 0.17$ [28]. Our computer simulations agree with these predictions (see figure 4).

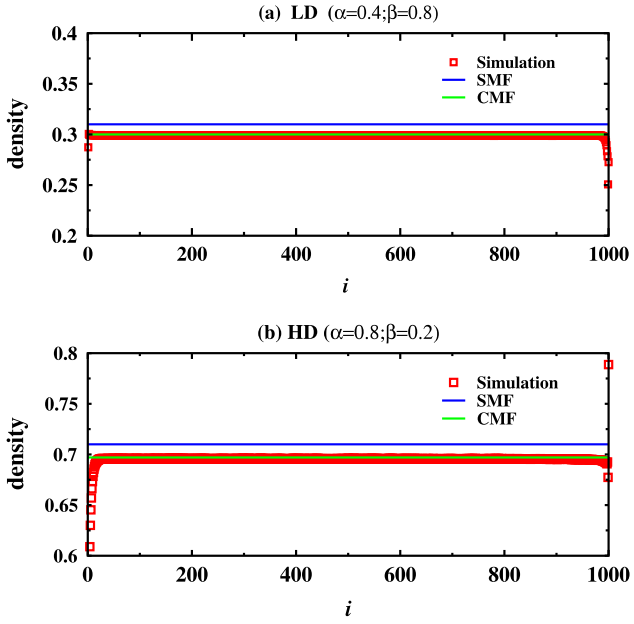

Figure 3. Density profiles for TASEP with inter-molecular interactions for $E = -1.2k_BT$. (a) The LD phase with $\alpha = 0.4$ and $\beta = 0.8$; (b) the HD phase with $\alpha = 0.8$ and $\beta = 0.2$.

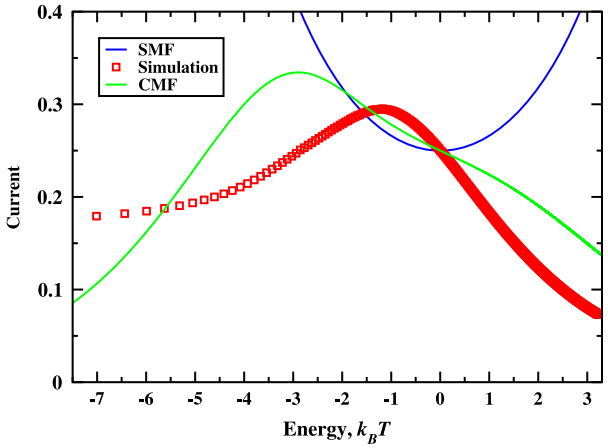

Figure 4. Maximal current as a function of the interaction strength. Lines are predictions from mean-field calculations. Symbols are from Monte Carlo computer simulations.

It is interesting to consider why the SMF provides a qualitatively reasonable picture of the phase diagram, while for particle currents it fails completely. The phase diagram is quantified by different particle densities, and for densities correlations are less important than for currents that are determined by the simultaneous occupancies of several neighboring lattice sites.

The theoretical framework of the CMF method, along with computer simulations, allows us to investigate the fundamental effect of interactions on the multi-particle dynamics in the TASEP model. It has been argued above that particle currents should diminish for strong

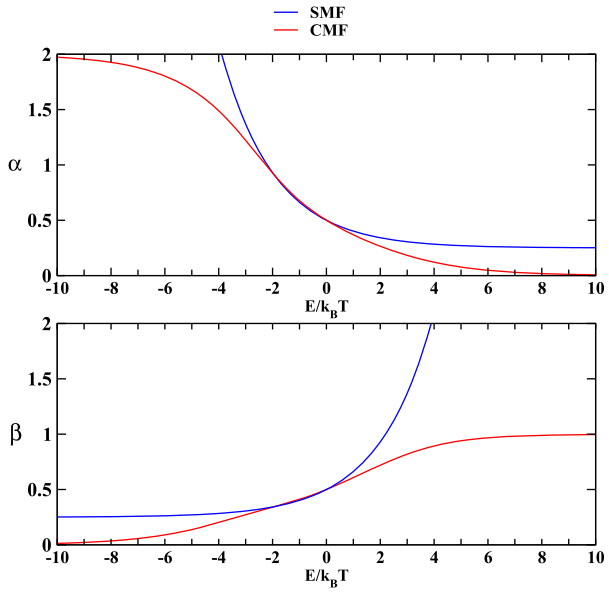

Figure 5. Coordinates of the triple points in phase diagrams as a function of the interaction strength. Lines correspond to predictions from two kinds of mean-field calculations. Symbols are results from computer simulations.

attractions and repulsions. This suggests that there is an intermediate strength of interactions where the maximal flux might be achieved. Our calculations support these arguments, as illustrated in figure 4. We found that this optimal strength corresponds to weak repulsions with $E^* \approx -3k_BT$ in the CMF, while the simulations indicate $E^* \approx -1.2k_BT$. The surprising observation is that optimal conditions do not correspond to the case of no interactions, as one would expected from naive symmetry arguments. These arguments indicate that for attractive interactions, the flux should be smaller because of particle clustering, while repulsions decrease the current by slowing the particles that are close to each other. In addition, the optimal particle flux can be larger than the current for the system with only hard-core exclusions. The computer simulations predict $J_{max} \approx 0.29$, which is 16% greater than the maximal current for TASEP without interactions: $J_{max} = 0.25$. Thus, inter-molecular interactions might significantly modify particle fluxes.

It could also be observed that the effect of interactions on the particle dynamics in TASEP is not symmetric with respect to $E = 0$. The results from the CMF calculations and the Monte Carlo computer simulations suggest that there is more sensitivity for attractive interactions. The phase diagram also depends on the sign and strength of the interactions. Figure 5 shows the position of the triple point (that connects the LD, HD and MC phases) for different values of E. One can see that increasing repulsions shrinks the MC and HD phases, and the LD phase occupies the largest fraction of the parameter space. For strong attractions, the result is opposite: the HD phase dominates, while the LD and MC phase significantly diminish. These observations can be easily explained. Repulsions decrease the effective rate of entrance into the system, making it a rate-limiting step for a larger range of parameters. This corresponds to expanding the LD phase. For attractions, the exit rate slows down significantly, because particles leaving the system should sometimes break from the clusters. This is not favorable from the energetic point of view. In this case, the HD phase dominates the system.

It is interesting to apply our theoretical analysis to real motor proteins. Experimental studies show that kinesin molecular motors bound to cytoskeleton filaments experience short-range attractive interactions of order $E = (1.6 \pm 0.5)\, k_B T$ [9]. Comparing this result with the plots in figure 4, we conclude that kinesins probably do not function in the most optimal regime with the maximal particle current. However, they operate under conditions where small changes in interactions might lead to large modifications in the dynamic properties. This suggests that kinesins might be optimized not for the maximal flux but for supporting robust cellular transport via tuning its inter-molecular interactions. This allows molecular motors to compensate for fluctuations due to collisions with other molecules and to external loads. We hypothesize that this collective dynamic behavior of kinesins might be the most efficient from the energetic point of view. This picture agrees with current views on mechanisms of cooperativity in multiple kinesins [5, 7]. However, we should note that our model of motor protein dynamics is oversimplified. It ignores many important processes such as back stepping, bindings to the filaments and unbindings from them, and hydrolysis. It is not clear what effect the inter-molecular interactions will have if all relevant chemical transitions are included.

4. Summary and conclusions

In conclusion, we have developed a new theoretical approach for investigating the effect of inter-molecular interactions on the dynamics of cellular molecular motors that move along cytoskeleton filaments. Our method is based on employing totally asymmetric simple exclusion processes that are known to be successfully used in the analysis of non-equilibrium multi-particle phenomena. The important part of the method is a thermodynamically consistent procedure that allowed us to quantitatively describe the effect of inter-molecular interactions. Theoretical calculations indicate that interactions bring about significant spatial correlations in the system that could be partially captured by considering the dynamics of clusters. It is found that there is an optimal strength of interactions for which the particle current reaches its maximum, while for large attractions or repulsions the fluxes disappear. For TASEP, these optimal conditions correspond to weak repulsions. This observation is unexpected since from naive symmetry arguments the case of no interactions seems to be optimal. Interactions also modify stationary phase diagrams. For repulsions, the LD phase becomes the most important, while for attractions, the HD phase dominates. Our analysis also shows that dynamic properties are more sensitive to attractive interactions. The implications of these observations for kinesin motor proteins are discussed. It is argued that kinesins might be functioning under conditions supporting the robustness of the cellular transport instead of the maximal fluxes. At the same time, it was noticed that our theoretical analysis does not account for several important transitions in motor proteins, which might limit its applicability in the current form. It will be important to extend our method to include these features and to test our theoretical predictions for other classes of motor proteins.

Acknowledgments

We acknowledge support from the National Institute of Health (grant 1R01GM094489-01) and from the Welch Foundation (grant C-1559). The partial support from the Center for Theoretical Biological Physics at Rice University is also acknowledged.

References

[1] Alberts B, Johnson A, Lewis J, Raff M, Roberts K and Walter P 2007 *Molecular Biology of the Cell* 5th edn (New York: Garland Science)
[2] Howard J 2001 *Mechanics of Motor Proteins and the Cytoskeleton* (Sunderland, MA: Sinauer Associates)
[3] Kolomeisky A B and Fisher M E 2007 *Annu. Rev. Phys. Chem.* **58** 675
[4] Chowdhury D 2013 *Phys. Rep.* **529** 1
[5] Kolomeisky A B 2013 *J. Phys.: Condens. Matter* **25** 463101
[6] Veigel C and Schmidt C F 2011 *Nature Rev. Mol. Cell Biol.* **12** 163
[7] Uppulury K, Efremov A K, Driver J W, Jamison D K, Diehl M R and Kolomeisky A B 2012 *J. Phys. Chem.* B **116** 8846
[8] Neri I, Kern N and Parmeggiani A 2013 *New J. Phys.* **15** 085005
[9] Roos W H, Campàs O, Montel F, Woehlke G, Spatz J P, Bassereau P and Cappello G 2008 *Phys. Biol.* **5** 046004
[10] Vilfan A, Frey E, Schwabl F, Thormahlen M, Song Y H and Mandelkow E 2001 *J. Mol. Biol.* **312** 1011–26
[11] Seitz A and Surrey T 2006 *EMBO J.* **25** 267
[12] Campàs O, Kafri Y, Zeldovich K B, Casademunt J and Joanny J F 2006 *Phys. Rev. Lett.* **97** 038101
[13] Pinkoviezky I and Gov N S 2013 *New J. Phys.* **15** 025009
[14] Slanina F 2008 *Eur. Phys. Lett.* **84** 50009
[15] Derrida B 1998 *Phys. Rep.* **301** 65
[16] Chou T, Mallick K and Zia R K P 2011 *Rep. Prog. Phys.* **74** 116601
[17] Bressloff P C and Newby J M 2013 *Rev. Mod. Phys.* **85** 135
[18] Parmeggiani A, Franosch T and Frey E 2003 *Phys. Rev. Lett.* **90** 086601
[19] Dong J J, Klumpp S and Zia R K P 2012 *Phys. Rev. Lett.* **109** 130602
[20] Golubeva N and Imparato A 2012 *Phys. Rev. Lett.* **109** 190602
[21] Tsekouras K and Kolomeisky A B 2008 *J. Phys. A: Math. Theor.* **41** 465001
[22] Klumpp S and Lipowsky R 2003 *J. Stat. Phys.* **113** 233
[23] Lipowsky R, Klumpp S and Nieuwenhuizen T M 2001 *Phys. Rev. Lett.* **87** 10101
[24] Klumpp S and Lipowsky R 2004 *Europhys. Lett.* **66** 90
[25] Antal T and Schütz G M 2000 *Phys. Rev.* E **62** 83
[26] Hager J S, Krug J, Popkov V and Schütz G M 2001 *Phys. Rev.* E **63** 056101
[27] Katz S, Lebowitz J L and Spohn H 1998 *J. Stat. Phys.* **34** 497
[28] Lakatos G and Chou T 2003 *J. Phys. A: Math. Gen.* **36** 2027
[29] Derbyshev A E, Poghosyan S S, Povolotsky A M and Priezzhev V B 2012 *J. Stat. Mech.* P05014
[30] Juhasz R 2007 *Phys. Rev.* E **76** 021117